Radiation Measurements 125 (2019) 7–14

Contents lists available at ScienceDirect

Radiation Measurements

journal homepage: www.elsevier.com/locate/radmeas

Thermoluminescence measurements of *in-vitro* and *in-vivo* aged porcelain

Ioanna K. Sfampa[a,*], Lamprini Malletzidou[b], Panagiotis Pandoleon[c], George Kitis[a]

[a] Nuclear and Elementary Physics Laboratory, School of Physics, Faculty of Sciences, Aristotle University of Thessaloniki, GR-54124, Thessaloniki, Greece
[b] Department of Solid State Physics, School of Physics, Faculty of Sciences, Aristotle University of Thessaloniki, GR-54124, Thessaloniki, Greece
[c] Department of Prosthodontics, Faculty of Dentistry, School of Health Sciences, Aristotle University of Thessaloniki, GR-54124, Thessaloniki, Greece

ARTICLE INFO

Keywords:
Thermoluminescence
Dental porcelain
Dosimetry
XRD
UV–Vis spectrophotometry

ABSTRACT

Radiation accidents led to the birth of an area in physics, accidental dosimetry. Thermoluminescence (TL) is a basic application tool in radiation dosimetry. Ceramic porcelain has been widely used in dentistry and is the most applied material as veneer layer in metal-ceramic restorations. The present work is aiming to prove this material as an accidental personal dosimeter. For this purpose, freshly prepared and *in-vitro* aged samples were examined, and the measurements were also applied in *in-vivo* aged samples which were collected from patients.

1. Introduction

Thermoluminescence (TL) is a basic application tool in radiation dosimetry, an area in Physics born in order to study and give insights to the consequences of radiation accidents. Its main application is on the determination of the absorbed dose due to radiation events, over and above the normal background radiation. Several materials have been studied as potential accidental dosimeters, such as building items (Bailiff et al., 2016). Among these materials, the attention is also focused on those which can be found in the anthropogenic environment, but also on those that are probable to be found on a person, or even assembled in a person; in the last category, human hair, teeth and nails are included, but biomaterials also, which are widely used in surgical and dentistry applications (Bailiff et al., 2016; Polymeris et al., 2017).

Porcelain has been widely used in dentistry and is the most applied material as veneer layer in metal-ceramic restorations. It has been used in dentistry restoration since 1789 and, in 1962, porcelain composed by feldspathic ceramics was firstly used by Weinstein et al. (1962) for metal-ceramic restorations. In the last category, feldspathic ceramics are generally consisted of feldspar, quartz, kaoline and other oxides (e.g. Li_2O, B_2O_3, MgO, P_2O_5) (Yamamoto, 1985).

The present work attempts to prove porcelain as an accidental personal dosimeter. For this purpose, freshly prepared samples and *in-vitro* aged were examined. The measurements were also applied in *in-vivo* aged samples, which were collected from patients. Although porcelain has been examined before as a potential material for accidental dosimetry, the majority of the relevant scientific works is referred only to laboratory prepared samples (Veronese et al., 2010; Geber-Bergstrand et al., 2012; Ekendahl et al., 2013; Ekendahl and Judas, 2017). It is a unique experiment that aims to collect information from both *in-vitro* and *in-vivo* aged samples and study thoroughly their dosimetric properties. Additionally, characterization analysis (X-Ray Diffractometry and UV–Vis spectrophotometry) was applied to every step of the aging, in order to record any potential structural changes of the material under study.

2. Materials and methods

2.1. Sampling

In the present work, ceramic specimens were fabricated from the veneering glass-ceramic IPS e.max Ceram by Ivoclar Vivadent AG. The specimens were prepared according to the production company's guidelines ("IPS InLine System, Instructions for Use, 2006"), and in two specimen groups, with and without glazing.

The *in-vitro* aging was achieved through a thermal cycling procedure. Thermocycling (TC) simulates the oral environment by causing artificially accelerated aging. This method includes standardized thermal variations in a humid environment with deionized water, which simulates the thermal variations developed within the oral cavity (Gale and Darwell, 1999; Wegner et al., 2002; D'Amario et al., 2010; Palla et al., 2018; Kelesi et al., 2018).

For TC, the specimens were subjected to repeated cycles of hot and cold, in water baths according to the following sequence: 5 °C–37 °C to 55 °C–37 °C. In total, 7300 cycles were performed as -according to Gale and Darwell (1999) - this number of cycles corresponds to one year of

* Corresponding author.
E-mail addresses: isfaba@physics.auth.gr (I.K. Sfampa), labrinim@auth.gr, lmale@physics.auth.gr (L. Malletzidou), ppandoleon@dent.auth.gr, ppandoleon@gmail.com (P. Pandoleon), gkitis@auth.gr (G. Kitis).

https://doi.org/10.1016/j.radmeas.2019.04.017
Received 21 October 2018; Received in revised form 14 April 2019; Accepted 16 April 2019
Available online 17 April 2019
1350-4487/

exposure in the oral cavity (Gale and Darwell, 1999; Palla et al., 2018; Kelesi et al., 2018).

In the present work, eight glass-ceramic groups of specimens were fabricated. Each group included 3 specimens, to enhance the accuracy of the measurements through repeatability. Half of them were left as-received, while the rest were glazed, simulating the standard clinical procedures. The specimens of the two different sets (as-received and glazed) were subjected to different aging time:

- Sample A: Zero aging
- Sample B: 7300 TC cycles, corresponding to 1 year of *in-vivo* aging
- Sample C: 14600 TC cycles, corresponding to 2 years of *in-vivo* aging
- Sample D: 21900 TC cycles, corresponding to 3 years of *in-vivo* aging

The in-vivo aged samples -which were studied during the present work-came from dental waste; old metal-ceramic restorations (crowns and bridges) were removed from patients because of their natural wear, in order to be replaced by new ones. The samples were in different stages of preservation and material loss; in some cases, only the metallic framework remained intact, with a minimum presence of the veneer material. According to the patients' statements, the collected dental restorations were placed 10–20 years ago. After their extraction, the dental restorations were cleansed and stored.

2.2. Characterization measurements

Characterization analysis of the samples was implemented by means of X-Ray Diffraction analysis (XRD) and Spectrophotometry (UV–Vis). The analysis was performed on the freshly prepared samples -glazed and unglazed-, and during of the stages of artificial aging of them, in order to examine the possible alterations of the material due to the aging process.

Phase identification of the components of the samples was performed by means of XRD, using a two-cycle Rigaku Ultima^{+} X-ray diffractometer, operating at 40 kV/30 mA, with CuK$_{\alpha}$ radiation, in Bragg-Brentano geometry (operating conditions: step 0.02°, count 1.5 s/step, range 5–90°). The collected XRD diffractograms were identified with JCPDS-ICDD ("PC Powder Diffraction Files, 2003").

UV–Vis measurements were performed with a PerkinElmer UV-VIS spectrophotometer, model Lambda 18, equipped with an integrating sphere, in reflectance mode, in the region of 200–800 nm, with a resolution of 1 nm. The optical band gaps were determined by applying the Kubelka - Munk equation and the Tauc plots on the collected diffuse reflectance spectra of the samples (Kubelka and Munk, 1931).

2.3. TL system

The TL System used for the thermoluminescence measurements is a Harshaw 3500 TLD-Reader, including only neutral density filters. The irradiations were applied through a ^{90}Sr/^{90}Y beta particle source, with a dose rate of 1.72 Gy/min. All measurements were performed in a nitrogen atmosphere, with a low constant heating rate of 2 °C/s, in order to avoid significant temperature lag. The samples were heated up to the maximum temperature of 400 °C.

3. Results and discussion

3.1. XRD measurements

In general, all the samples present the amorphous glass matrix form, which is the characteristic of porcelain (Fig. 1). The glass matrix form is dominant in all of the samples -unglazed and with the additional glazing. Additionally, there are indications of the phase of fluorapatite in the unglazed specimens, because of the 2-theta peak at 31.9°, which corresponds to the major (2 1 1) crystal lattice plane diffraction of fluorapatite ("PC Powder Diffraction Files," 2003). The fluorapatite -in nano-dimensions- is an additive of the porcelain under study (Bühler-Zemp and Völkel, 2005). The phase of fluorapatite is also present in the diffractograms of the glazed specimens after their in-vitro aging (Fig. 1c, as representative of the glazed and unglazed specimens after the in-vitro aging). Its presence is attributed to the gradual wear and decay of the superficial glazing.

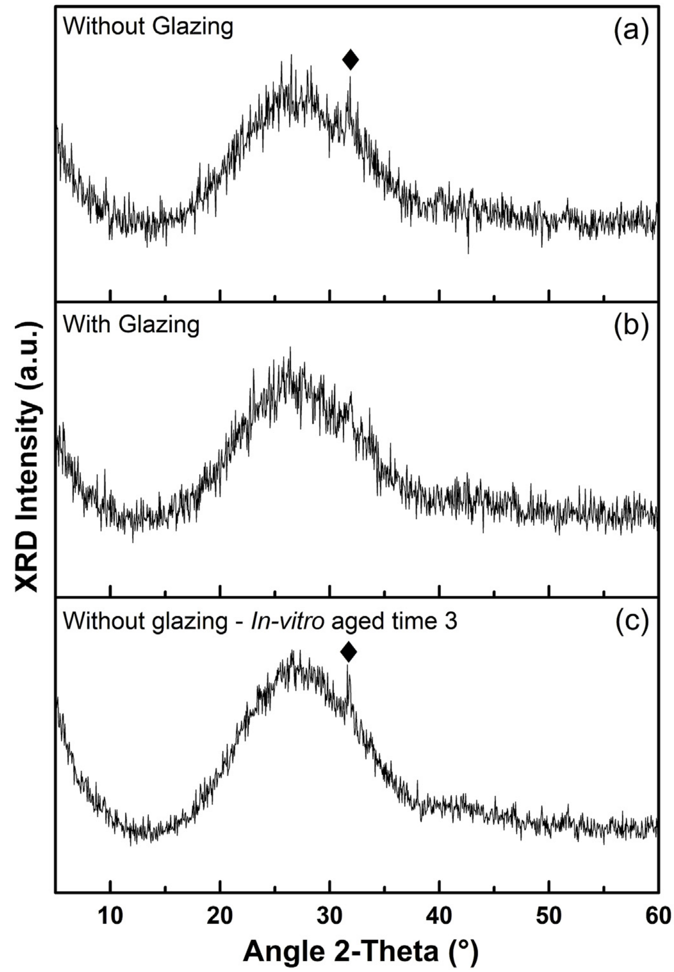

Fig. 1. Bragg-Brentano XRD patterns of porcelain samples; (a) and (b) correspond to the initial and without aging samples, without glazing and with glazing, respectively. The XRD pattern namely (c) is representative of the in-vitro aged samples, both with and without glazing (◆ fluorapatite hexagonal #15–0876, identification with JCPDS-ICDD).

3.2. UV–Vis measurements

Fig. 2 presents the diffuse reflectance spectra (a and c) and their Tauc plots (b and d) of the groups of glazed and unglazed specimens, for the specimens as-received and for all the in-vitro aging periods. All the samples present similar values of the optical band gap, of (3.45 ± 0.36) eV, with no significant difference regarding the aging time or the presence of glazing. The estimated optical energy gap implies that a trap appropriate for dosimetry could be present. On the other hand, the gap is narrow enough, so it ensures that no very deep traps (VDT) are present.

3.3. TL measurements on the porcelain specimens

Several protocols were applied to the samples. The results revealed the TL properties of both the glazed and un-glazed porcelain specimens, combined with the different *in-vitro* aging times. Furthermore, *in-vivo*

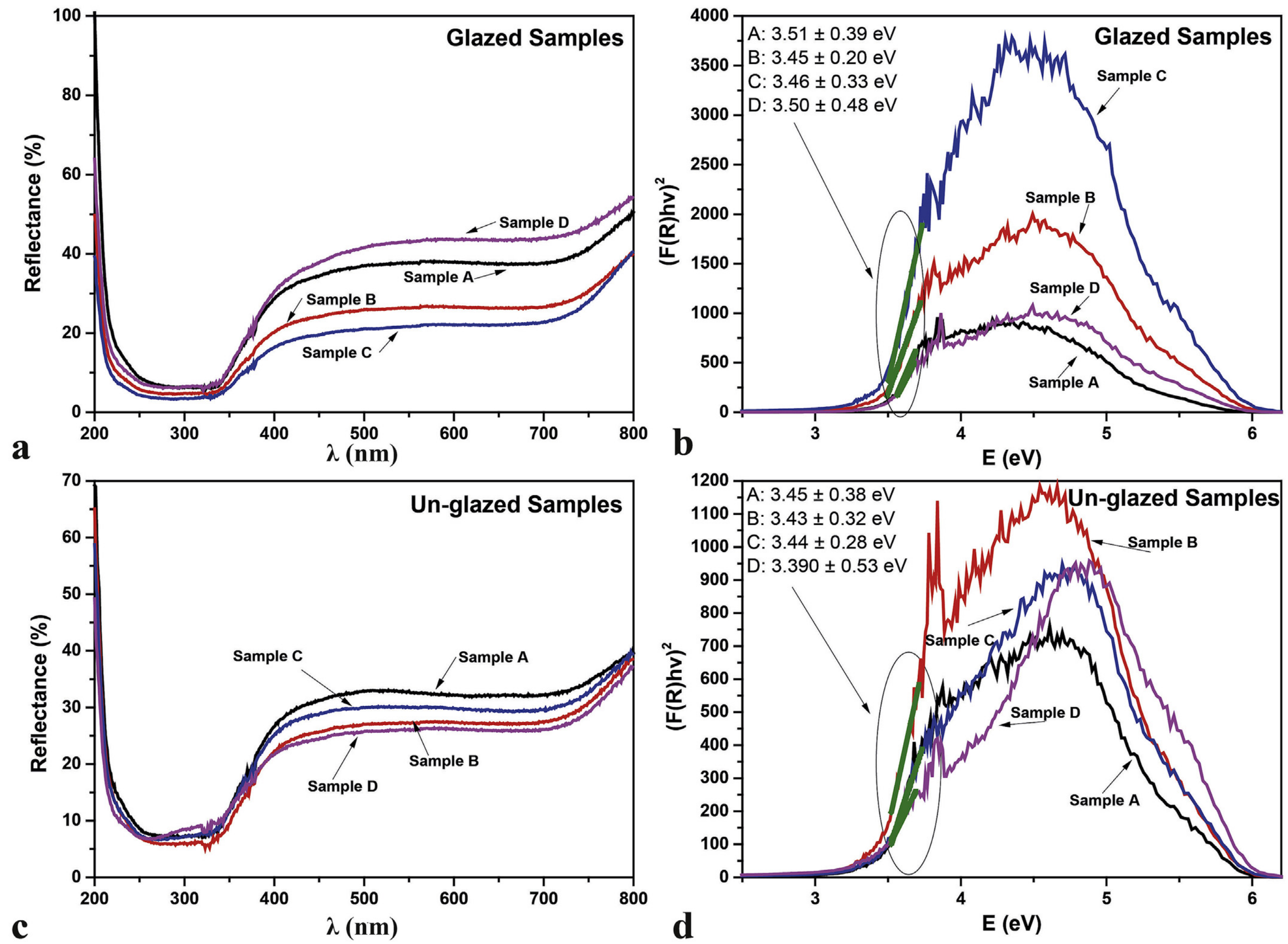

Fig. 2. Diffuse reflectance spectra (a, c) and Tauc plots with the applied linear fittings (b, d) for the determination of the optical band gaps of the samples. The calculation of the optical band gaps was applied in the noted linear regions of the Tauc plots within the ellipsoids.

aged samples were studied in order to be compared to the corresponding *in-vitro* aged specimens.

3.3.1. *The shape of the TL glow curve and sensitivity changes*

The preliminary thermoluminescence measurements on porcelain showed that the glow curve consists basically of two main glow peaks, as it is shown by the TL glow curves of the successive cycles of irradiation-measurement in Fig. 3. The first one is a low temperature peak around (120 ± 5) °C. The other one is a high temperature peak at (260 ± 10) °C. The high temperature peak is suitable for dosimetric applications, while the low temperature peak shows characteristics which seem to be suitable for estimating the time elapsed from the end of irradiation (medical irradiation or accidental incident related to ionizing irradiation).

The successive cycles of irradiation and TL measurement reveal that there are no significant differences in the shape and the intensity of the glow curve (Fig. 3). Specifically, ten successive cycles of irradiation (17 Gy) and heating up to 400 °C were carried out in order to investigate this behavior. These results imply that all the several experimental protocols are applicable also in single aliquot. Single aliquot protocols are the easiest to use in case of accidental dosimetry, especially in the case where only small amounts of sample are available. This last statement is of great importance in the case of biomaterials -including dental restorations-in order to minimize the invasion of the procedure.

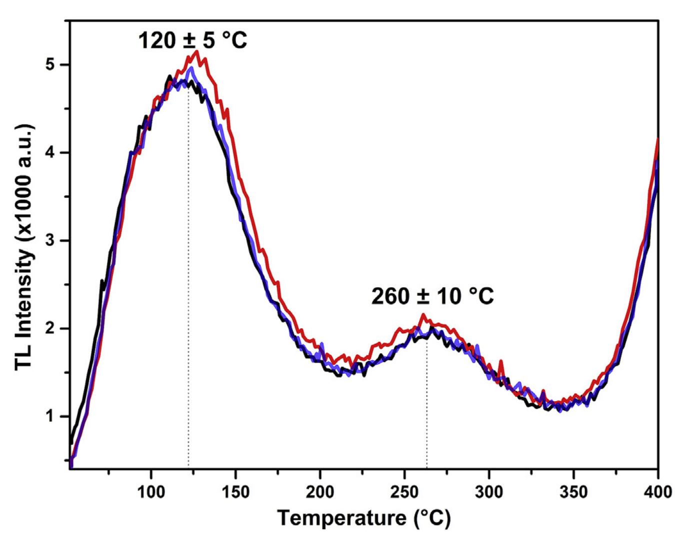

Fig. 3. TL glow curves of a porcelain specimen after the 1st, 5th and 10th successive cycles of irradiation-measurement, as representative of the successive measurements process. The shape and the intensity of the curves are similar for all the successive cycles, and independent of their state (glazed and unglazed specimens, as-received and in-vitro aged).

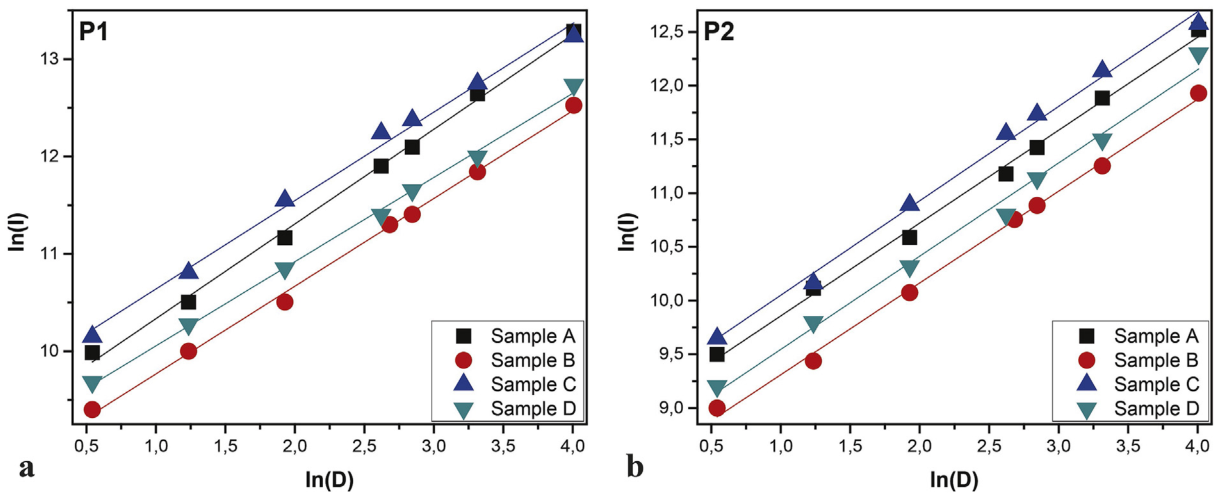

Fig. 4. Dose response of the samples A, B, C and D, for both peak 1 (P1) and peak 2 (P2). The data points were linearly fitted and the slopes are equal to 1 ± 0.05. The errors of the integrals are less than 2%.

3.3.2. Dose response and recovery test

The dose response protocol was performed for seven different doses between 1 and 55 Gy; all samples showed similar response to the different doses. As it is displayed in Fig. 4, both TL peaks show linear dependence over dose. Moreover, the linear fittings over the dose response measurements show that the slopes are equal to 1 ± 0.05 for all the groups of specimens under examination, and for both the TL peaks. The linear response to the doses is the most important property for a potential dosimeter.

The second TL peak, at ~260 °C, which corresponds to a deeper trap, is more probable of being stable in comparison with the first TL peak, at ~120 °C. For this reason, a dose recovery test was applied only to the second TL peak, as it is considered as more efficient to be used as a dosimetric peak. The dose recovery test of the second peak was applied according the protocol used by Duller (2008) and Wintle and Murray (2006).

After zeroing of its signal, the aliquot was irradiated with a known dose; in our case, this dose was settled on 5.16 Gy. This particular dose –of 5.16 Gy-was afterwards used as the "unknown" irradiation dose. Afterwards, the single aliquot regenerative dose (SAR) protocol was applied, which comprises subsequent cycles of irradiation with a different dose each time (D_i = 1.72, 3.44, 6.88, 12.04, 13.76 and 20.64 Gy and finally repeating the dose of 1.72 Gy for checking the recycling ratio), followed by a TL measurement up to 400 °C (L_i). In the second half of each cycle, the aliquot was irradiated with a test dose of 8.6 Gy, and then the TL signal (T_i) was recorded. The procedure was applied in 3 aliquots, for repeatability reasons.

Fig. 5 illustrates the corrected luminescence signal (L_i/T_i) as a function of the applied irradiation dose. Each data point represents the mean value of the three measured aliquots. The recycling ratio is equal to 0.99 ± 0.01, which is a value really close to the ideally value of 1. The "unknown" dose can then be calculated and it is found equal to (5.6 ± 0.1) Gy. The final calculated ratio of the recovery dose test is: 5.16 Gy/5.6 Gy ≈ 0.92, which is acceptable for using a sample of a particular material for dosimetry.

3.3.3. TL fading

In order to examine the fading of the TL signal after the storage of the specimens in dim conditions, in association with the storage time period, the following protocol was applied:

- Step 1: Irradiation with a Test Dose (TD) of 27 Gy and subsequent TL measurement to obtain the initial sensitivity.
- Step 2: TD and storage in dark for t_i = 2, 15, 26 and 50 h.

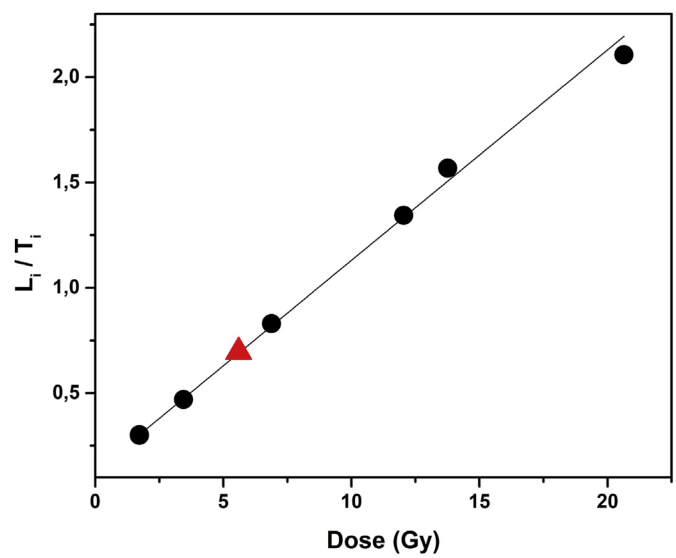

Fig. 5. The single aliquot regenerative dose (SAR) procedure applied to porcelain. The known doses are annotated with cycle symbols, while the triangle symbol represents the "unknown" dose. The growth of signal with dose is characterized by administering a number of laboratory doses of different values and measuring the resulting signals L_i. After each measurement, the luminescence sensitivity was measured by giving a fixed dose (here 8.6 Gy) and recording the resulting signal T_i. The effect of changes in sensitivity can be corrected by taking the ratio of the luminescence signal (L_i) to the response to the fixed dose (T_i). The plot of the sensitivity-corrected TL (L_i/T_i) as a function of the laboratory dose can be used to calculate the recovery dose for that aliquot. The errors were estimated < 1%.

- Step 3: Residual TL (RTL) measurement up to 400 °C for measuring the faded TL signal, while emptying at the same time all electron traps which were thermally activated below that temperature.

Fig. 6 illustrates the RTL glow curves according to the fading protocol. The second TL peak remains almost stable, at least for the first two days. This result is of great importance, as the period of the first two days is regarded as crucial, in case of an accident connected with ionizing irradiation.

On the contrary, the first peak is regarded as possible to be used in order to estimate the time elapsed since the accident. In this direction, the remnant signal of the first peak was treated according to the procedure described by Polymeris et al. (2006). Fig. 7 shows the fading of

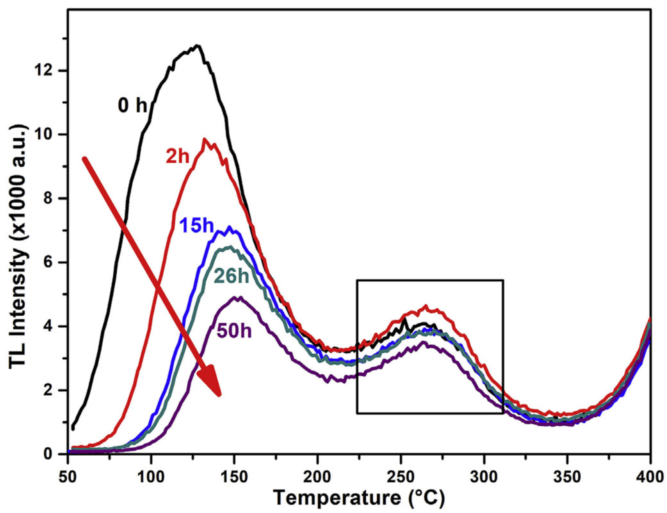

Fig. 6. RTL glow curves according to the applied fading protocol. The arrow indicates the decrease of P1 as a function of the fading time.

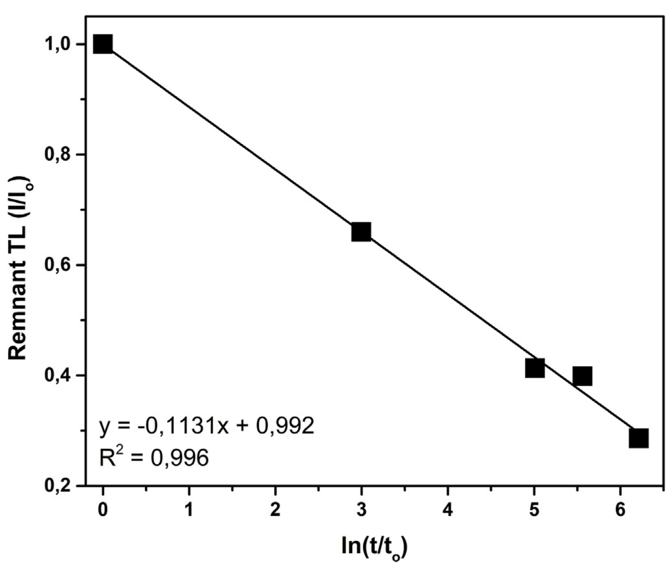

Fig. 7. Fading of the TL signal. RTL vs ln(t/t$_o$) presents a linear tendency (time is expressed in hours). The solid line presents the linear fitting according to the linear equation while the fitting parameters are also displayed.

the TL signal of the first peak; the data points are fitted with a linear equation according to the following form:

$$r = A - K \cdot \ln\left(\frac{t}{t_o}\right) \quad [3.1]$$

where $A \cong 1$, $K = (\ln(t_m/t_o))^{-1}$, t_m is the maximum time for which the tunneling mechanism holds, and t_o is the short period of time between the end of the irradiation and the measurement. As it is displayed in Fig. 7, the linear fitting presents a slope of 0.1131 and an intercept of 0.992. Thus, Eq. (3.1) is written as:

$$r = 0.992 - 0.1131 \cdot \ln\left(\frac{t}{t_o}\right) \quad [3.2]$$

3.3.4. Lower detection limit

The Lower Detection Limit (D_{LDL}) was calculated under the procedure described by Pagonis et al. (2006). According this procedure, the D_{LDL} is defined as three times the standard deviation (σ_{bg}) of the zero dose reading, given in Gy.

- The average of the zero dose readings is equal to 128 a.u., with a standard deviation of 10 a.u.
- The calibration factor of the TL reader is given by the calibration dose (1.72 Gy) divided by the average value of 24 TL readings (equal to the 8 groups × 3 specimens), and the result is (5.55 ± 0.43) mGy/a.u.
- Finally, the calculated D_{LDL} is equal to: D_{LDL} = (3 × 10) × 5.55 ≃ 0.2 Gy, for a sample of mass comparable to the mass of LiF: Mg, Ti (TLD-100) (25 mg, chip).

This evaluated D_{LDL} value is considered as promising for using dental porcelain as a proper material for accidental dosimetry.

3.3.5. Isothermal decay

The experimental procedure for the Isothermal Decay study of TL (ITL) was performed according to the following protocol:

- Step 1: The previously annealed aliquot was irradiated with TD = 25 Gy, in order to populate the traps and centers.
- Step 2: TL measurement up to a temperature T with a step of 2 °C/s. At this temperature, called T_{dec}, the sample was left to decay thermally for 100 s.
- Step 3: After the end of the decay period, the sample was cooled down to room temperature and then measured up to T = 400 °C.
- Step 4: The steps 1–3 were repeated for a new decay temperature T_{dec}.

T_{dec} is at the range of 80–150 °C with a step of 10 °C. These temperatures are connected with the temperature range of the first glow peak.

Fig. 8 shows that the normalized curves almost coincide; there is only a slight difference between them, independent on the stimulation temperature. This kind of results is considered as a typical behavior for tunneling recombination processes at elevated temperatures (Sfampa et al., 2014). All the obtained experimental data were analyzed by applying a de-convolution approach. In the computerized curve deconvolution analysis of ITL, the goodness of fit was tested by the figure of merit (FOM) of Balian and Eddy (1977). Microsoft Excel along with the Solver add-on feature (Afouxenidis et al., 2012) is being utilized for all curve fittings.

The recorded curves from this experiment were analyzed and fitted through the following analytical equations (Kitis and Pagonis, 2013):

$$I(t) = \frac{C[F(t)]^2}{1 + zAt} \cdot \exp(-\rho'[F(t)]^3) \quad [3.3]$$

$$F(t) = ln(2.718 + zAt) \quad [3.4]$$

where C is a constant related to the initial concentration of trapped electrons, and the quantity A (s^{-1}) represents the stimulation probability for the ITL stimulation process. The stimulation probability can also be described as $A = 1/\tau$, where τ is the characteristic time constant for each stimulation mode, and *I(t)* represents the intensity of the signal as a function of time. The time parameter in the case of ITL represents the duration of the isothermal experiment. In this equation, ρ' is the dimensionless concentration of charge carriers and $z = 1.8$ is a constant. Regarding the ITL experiments, $A = s \cdot \exp(-E/kT)$, where T is the constant temperature, E the activation energy, s is a frequency factor and k is the Boltzmann constant.

An example of the fitting procedure is presented in Fig. 9. One tunneling component plus a linear long-lived component were able to fit the experimental data. All the data for each sample were fitted according to the aforementioned procedure.

3.3.6. Estimation of activation energy

In order to reveal more information about the glow curve, two different ways were followed. Firstly, the initial rise (IR) method was

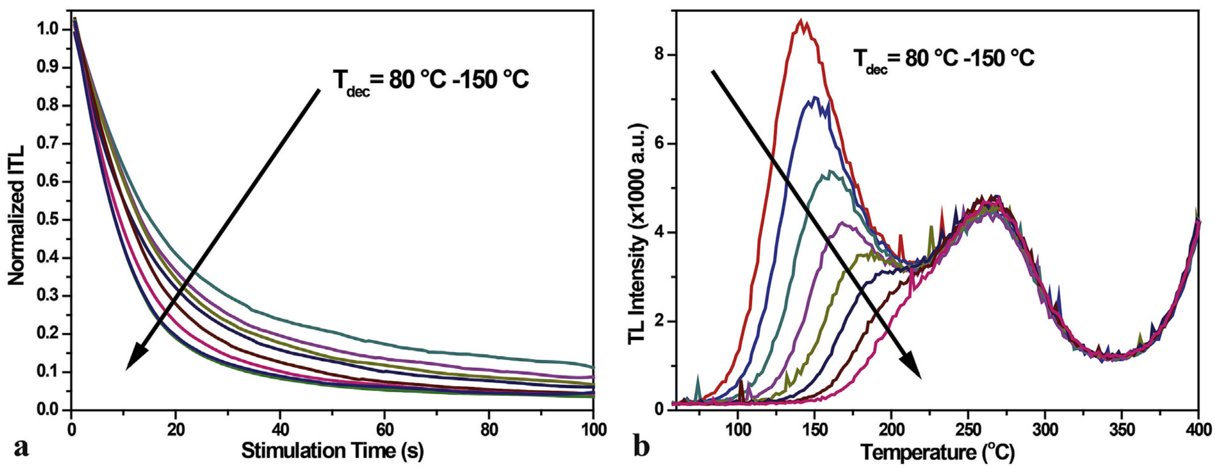

Fig. 8. ITL curves (a) and corresponding residual TL glow curves (b). The arrows indicate the change of the curve as a function of the decay temperature.

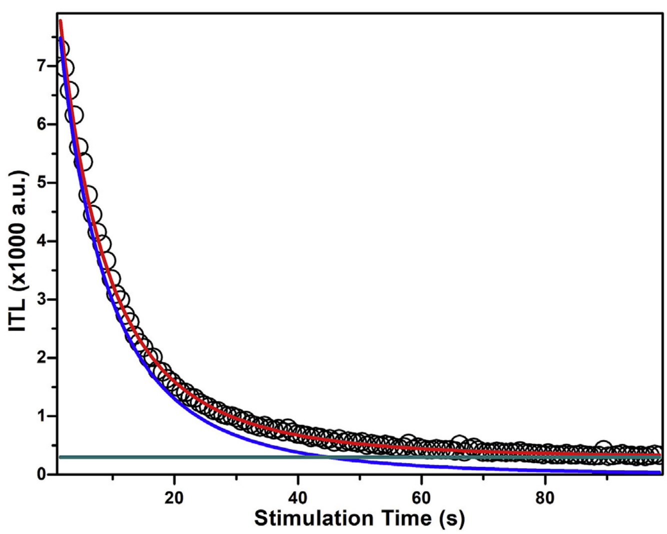

Fig. 9. An example of the fitting procedure according to equations [3.1]-[3.2] for the sample A. The black circles represent the experimental data, while the red line is the sum of the fitted components (blue line corresponds to the tunneling component and green line corresponds to the linear long-lived component). (For interpretation of the references to colour in this figure legend, the reader is referred to the Web version of this article.)

applied, as described by Chen and McKeever (1997). The IR method is the most valuable technique for the evaluation of the activation energy of an electron trap responsible for a TL peak. The method was introduced by Garlick and Gibson (1948) and a generalized version of the initial rise method named fractional glow technique has been presented by Gobrecht and Hofmann (1966). The method was applied to one specimen of each group of samples (glazed, unglazed, initial and in-vitro aged); the calculated values of the activation energies showed differentiations no bigger than 10%. In Fig. 10a, the mean values of the calculated energies are illustrated, as a function of temperature. The results show that the first peak corresponds to a trap with an energy of (1.15 ± 0.1) eV, while the second peak corresponds to a trap with an energy of (1.3 ± 0.1) eV.

Then, the glow curves were analyzed through a deconvolution method of analysis, using the general kinetic order model (GOK) for all of the specimens under study (Kitis et al., 1998). In Fig. 10b, a representative example of the deconvolution method is presented, as no differentiations greater than 5% were observed in the calculated activation energies. Microsoft Excel along with the Solver add-on feature (Afouxenidis et al., 2012) was utilized for the deconvolution. Six peaks were used in total and the evaluated energies for the most prominent of them are (1 ± 0.05) eV (at 120 °C) and (1.2 ± 0.05) eV (at 270 °C).

It is assumed that both methods conclude to similar results. Additionally, Fig. 10b reveals -through the applied deconvolution-that the glow-curve is complex, as it consists of more than one overlapping TL peaks.

3.4. TL properties of the in-vivo aged samples

Preliminary experimental protocols were also applied in samples collected from patients. Fig. 11 presents representative examples of the TL measurements applied to the collected *in-vivo* aged samples. Nine metal-ceramic restorations were collected and -according to the patients' medical records-the samples were between 15 and 20 years old.

Five of the samples presented similar results and many similarities to the previously examined *in-vitro* aged porcelain samples; in Fig. 11a, a representative example of this group (vv1) is presented. The same peaks, as in the case of *in-vitro* aged, were also recorded for these samples; P1 is located at about (120 ± 5) °C, and P2 at about (260 ± 10) °C (Fig. 11a). Furthermore, the experimental protocol about the dose response revealed that the *in-vivo* aged samples presented the same behavior as the *in-vitro* aged samples. The results agree to the conclusion that the *in-vitro* and *in-vivo* aged samples follow the same patterns in case of the same protocols.

Additionally, two of the samples (vv2) presented a slightly altered shape of their TL glow curve. As it is illustrated in Fig. 11b, in this case, the collected TL glow curves also present a peak suitable for dosimetry, at ~340 °C.

Finally, it was impossible to apply the same experimental procedures to the two remaining of the *in-vivo* aged samples, because of their state of preservation. In this case, only flakes of the veneer material remained intact on the metallic frameworks, making it impossible to collect enough material for study.

As it is displayed in Fig. 12, both the *in-vivo* samples' groups (namely vv1 and vv2) show linear dependence over the irradiation dose. Moreover, the linear fittings over the dose response measurements show that the slopes are equal to 0.95 ± 0.05 for all the groups of specimens under examination.

The main drawback of the porcelain is that it presents photosensitivity. This will be the subject for future work, since it would insert special treatment during the collection from the patients. Moreover, that implies that the OSL properties should be also examined thoroughly.

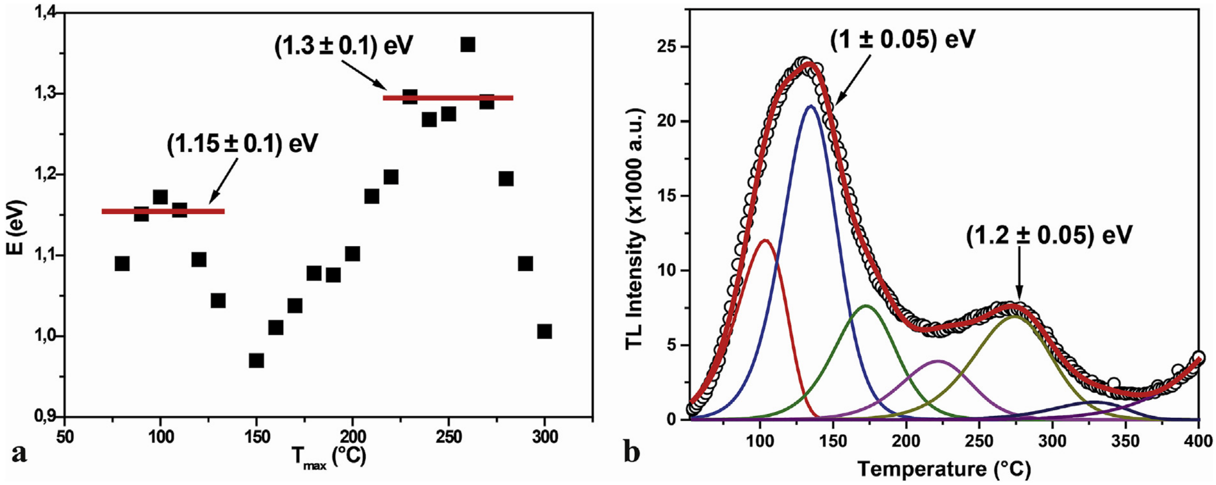

Fig. 10. Evaluation of the activation energies of the samples according to the initial rise method (a) and the deconvolution method of analysis using the GOK model (b). Regarding the initial rise method, the mean values of the calculated energies are plotted vs temperature. The notated energies correspond to the mean value of the activation energies calculated for all of the specimens under examination. In the case of the deconvolution method, the analysis of an unglazed specimen of group A is illustrated, as representative, irradiated with a dose of 55 Gy.

4. Conclusions

4.1. Dosimetric properties

- The samples presented repeatability over the successive cycles of irradiation-measurement. This fact implies that the applied protocols are also applicable for single aliquot procedures.
- Linear response to the different doses was present for both *in-vitro* and *in-vivo* aged samples.
- Through the first peak and the calculated decay time, the time elapsed since the radiation event is possible to be estimated.
- The lower detectable limit (D_{LDL}) of irradiation was estimated at 0.2 Gy, for a sample of mass comparable to the mass of LiF, which is one of the most widely used TLDs.
- Regarding the *in-vivo* examined samples, the results implied that there is a wide range of materials which used to be applied for dental restorations (different brands of porcelain with unknown additives). The promising part is that all the samples present at least one peak prominent for dosimetric applications.

4.2. Contribution to the TL mechanism

- The first peak presented clearly tunneling recombination mechanism.
- The estimated band gap of only 3.5 eV ensured the absence of very deep traps (VDT) which offers a possibility of testing models based on strong competition from VDT.

4.3. Future work

Further work should involve a wider range of porcelain brands in order to ensure the dosimetric properties of porcelain in general. This aspect will empower the results of the *in-vivo* aged samples, since it is difficult to collect information about the kind of used porcelain, especially for dental restorations older than 10 years. Moreover, the preliminary measurements that imply the presence of photosensitivity will be examined thoroughly.

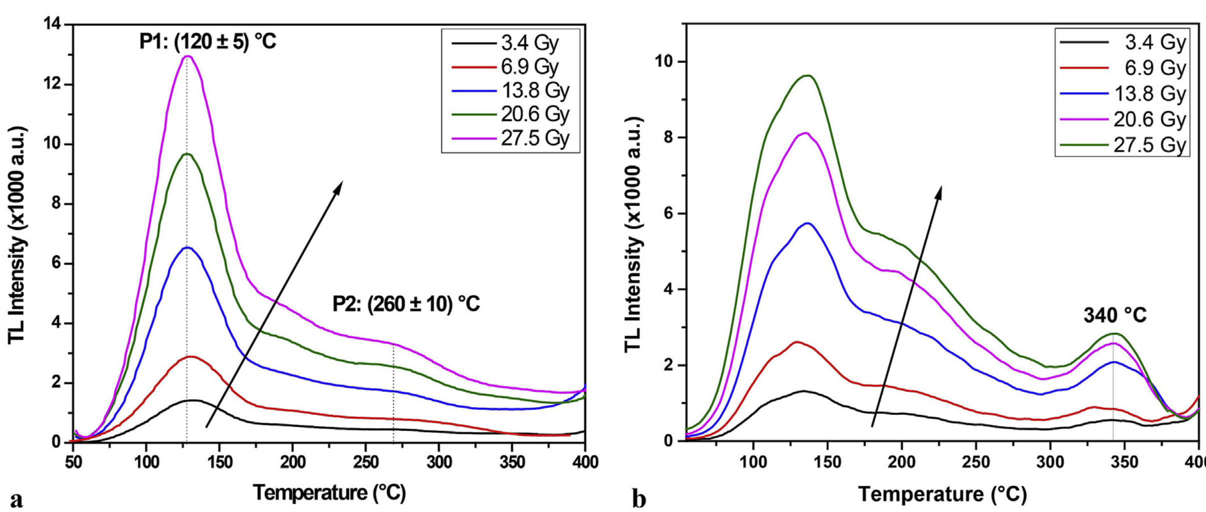

Fig. 11. Representative dose response glow curves of the two different groups of the in-vivo aged samples. The majority of the collected samples present the same behavior with the in-vitro aged specimens (vv1) (a). Two of the in-vivo aged samples under examination showed a differentiation of the glow curves, with an additional peak at ∼340 °C (vv2) (b). The arrows indicate the raise of the TL signal after the irradiation with higher dose.

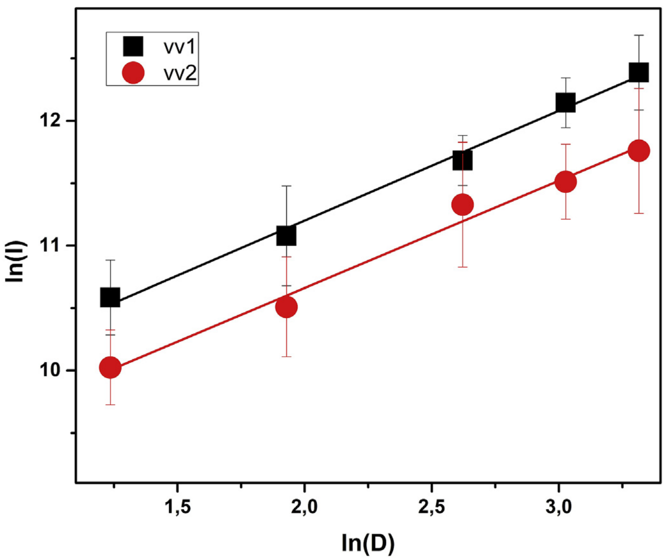

Fig. 12. Dose response of the groups vv1 and vv2. The data points were linearly fitted and the slopes are equal to 0.9 ± 0.05. The errors of the integrals are < 5%.

Acknowledgments

This project is implemented through the Operational Program "Human Resources Development, Education and Lifelong Learning" and is co-financed by the European Union (European Social Fund) and Greek national funds (MIS Code: 5004727).

Appendix A. Supplementary data

Supplementary data to this article can be found online at https://doi.org/10.1016/j.radmeas.2019.04.017.

References

Afouxenidis, D., Polymeris, G.S., Tsirliganis, N.C., Kitis, G., 2012. Computerized curve deconvolution of TL/OSL curves using a popular spreadsheet program. Radiat. Protect. Dosim. 149, 363–370. https://doi.org/10.1093/rpd/ncr315.

Bailiff, I.K., Sholom, S., McKeever, S.W.S., 2016. Retrospective and emergency dosimetry in response to radiological incidents and nuclear mass-casualty events: a review. Radiat. Meas. 94, 83–139. https://doi.org/10.1016/j.radmeas.2016.09.004.

Balian, G.H., Eddy, N.W., 1977. Figure-of-merit (FOM), an improved criterion over the normalized chi-squared test for assessing goodness-of-fit of gamma-ray spectral peaks. Nucl. Instrum. Methods 145, 389–395. https://doi.org/10.1016/0029-554X(77)90437-2.

Bühler-Zemp, P., Völkel, T., 2005. IPS e.max ® Ceram Scientific Documentation.

Chen, R., McKeever, S.W.S., 1997. Theory of Thermoluminescence and Related Materials. World Scientific, Singapore.

D'Amario, M., Campidoglio, M., Morresi, A.L., Luciani, L., Marchetti, E., Baldi, M., 2010. Effect of thermocycling on the bond strength between dual-cured resin cements and zirconium-oxide ceramics. J. Oral Sci. 52, 425–430.

Duller, G., 2008. Luminescence Dating Guidelines on Using Luminescence Dating in Archaeology. English Heritage, Swindon.

Ekendahl, D., Judas, L., Sukupova, L., 2013. OSL and TL retrospective dosimetry with a fluorapatite glass-ceramic used for dental restorations. Radiat. Meas. 58, 138–144. https://doi.org/10.1016/j.radmeas.2013.01.001.

Ekendahl, D., Judas, L., 2017. OSL and TL retrospective dosimetry with leucite glass-based dental ceramics. Radiat. Meas. 104, 1–7. https://doi.org/10.1016/J.RADMEAS.2017.06.013.

Gale, M.S., Darwell, B.W., 1999. Thermal cycling procedures for laboratory testing of dental restorations. J. Dent. 27, 89–99.

Garlick, G.F.J., Gibson, A.F., 1948. The electron trap mechanism of luminescence in sulphide and silicate phosphors. Proc. Phys. Soc. 60, 574–590 Article number 308.

Geber-Bergstrand, T., Bernhardsson, C., Mattsson, S., Rääf, C.L., 2012. Retrospective dosimetry using OSL of tooth enamel and dental repair materials irradiated under wet and dry conditions. Radiat. Environ. Biophys. 51, 443–449. https://doi.org/10.1007/s00411-012-0434-9.

Gobrecht, H., Hofmann, D., 1966. Spectroscopy of traps by fractional glow technique. J. Phys. Chem. Solids 27, 509–522. https://doi.org/10.1016/0022-3697(66)90194-6.

IPS InLine System, 2006. Instructions for use. https://doi.org/10.1515/9783110824469.X.

Joint Committee on Powder Diffraction Standards, 2003. PC Powder Diffraction Files International Centre for Diffraction Data (PC PDF, JCPDS-ICDD).

Kelesi, M., Kontonasaki, E., Kantiranis, N., Papadopoulou, L., Zorba, T., Paraskevopoulos, K.M., Koidis, P., 2018. The effect of different aging protocols on the flexural strength and phase transformations of two monolithic zirconia ceramics. J. Appl. Mater. Funct. Mater in press.

Kitis, G., Gomez Ros, J.M., Tuyn, J.W.N., 1998. Thermoluminescence glow– curve deconvolution function for first, second and general order kinetics. J. Phys. D Appl. Phys. 31, 2636–2641.

Kitis, G., Pagonis, V., 2013. Analytical solutions for stimulated luminescence emission from tunneling recombination in random distributions of defects. J. Lumin. 137, 109–115.

Kubelka, P., Munk, F., 1931. Ein beitrag zur optik der farbanstriche. Zeitschrift für Technische Physik 12, 593–601.

Pagonis, V., Kitis, G., Furetta, C., 2006. Numerical and Practical Exercises in Thermoluminescence. Springer-Verlag, New York. https://doi.org/10.1007/0-387-30090-2.

Palla, E.S., Kontonasaki, E., Kantiranis, N., Papadopoulou, L., Zorba, T., Paraskevopoulos, K.M., Koidis, P., 2018. Color stability of lithium disilicate ceramics after aging and immersion in common beverages. J. Prosthet. Dent 119, 632–642. https://doi.org/10.1016/j.prosdent.2017.04.031.

Polymeris, G.S., Tsirliganis, N., Loukou, Z., Kitis, G., 2006. A comparative study of the anomalous fading effects of TL and OSL signals of Durango apatite. phys. stat. sol. (a) 203 (3), 578–590. https://doi.org/10.1002/pssa.200521347. 2006.

Polymeris, G.S., Giannoulatou, V., Kyriakidou, A., Sfampa, I.K., Theodorou, G., Şahiner, E., Meriç, N., Kitis, G., Paraskevopoulos, K.M., 2017. Bioactivity characterization of 45S5 bioglass using TL, OSL and EPR: comparison with the case of 58S sol-gel bioactive glass. Mater. Sci. Eng. C 70, 673–680. https://doi.org/10.1016/j.msec.2016.09.051.

Sfampa, I.K., Polymeris, G.S., Tsirliganis, N.C., Pagonis, V., Kitis, G., 2014. Prompt isothermal decay of thermoluminescence in an apatite exhibiting strong anomalous fading. Nucl. Instrum. Methods Phys. Res. B 320, 57–63.

Veronese, I., Galli, A., Cantone, M.C., Martini, M., Vernizzi, F., Guzzi, G., 2010. Study of TSL and OSL properties of dental ceramics for accidental dosimetry applications. Radiat. Meas. 45, 35–41. https://doi.org/10.1016/j.radmeas.2009.11.005.

Wegner, S.M., Gerdes, W., Kern, M., 2002. Effect of different artificial aging conditions on ceramic-composite bond strength. Int. J. Prosthodont. (IJP) 15, 267–272.

Weinstein, M., Weinstein, L.K., Katz, S., Weinstein, A., 1962. Fused porcelain-to-metal teeth. US Patent 3 052 982.

Wintle, A.G., Murray, A.S., 2006. A review of quartz optically stimulated luminescence characteristics and their relevance in single-aliquot regeneration dating protocols. Radiat. Meas. 41, 369–391. https://doi.org/10.1016/J.RADMEAS.2005.11.001.

Yamamoto, M., 1985. Metal Ceramics. Principles and Methods, second ed. Quintessence Publishing Co. Inc, Chicago 1985.